Investigate the Crashworthiness of high velocity bird impact on three different designed model wings by using Coupled Eulerian-Lagrangian approach

Abstract

Bird strike is a significant threat to the parts of the flying aircrafts. The wing is a central part, which provides stability to the aircraft. Mostly at wing, bird attack the leading edge. Worldwide aviation regulation FRA, EASA, required 4lb bird strike on the wing of aircraft, and after this bird strike, aircraft is able to be safely landed. This study aims to investigate the resistance of the wing against the bird strike and damage analysis of the high-velocity bird collision on the model wing, inner structure, spar, and ribs. By using the Coupled Eulerian-Lagrangian (CEL) approach in ABAQUS/Explicit. Our contribution 1) bird strike on a wing with assembled inner structure by aluminium and outer skin composed of unidirectional fiber-reinforced composite material. 2) bird strike on-wing which is similar with the first test in which the difference is of spar designed layers of horizontal plates like a comb. 3) bird strike on-wing which is similar with second model wing difference in this wing put an aluminium leading edge on the skin leading-edge, final to analyze the damage of bird impact on the wing, the velocity of bird strike is 200m/s and analyze the behavior of the bird at this velocity. Resistance behavior of composite skin After penetration in the wing, analyze the impact on the spar and stress on the inner structure. Analysis of the kinetic and internal energy graph and Comparison all of these results and check the performance, which gives an excellent result at this velocity. based on these results suggest which inner part is sensitive.

Keywords: Aluminium alloys, Bird strike, Composites, Impact fracture, Finite element analysis, Damage,

Introduction

since last two decades, one of the most popular ways of traveling is through airlines. It is safer and faster than any other means of traveling. In wars, military aircraft plays a leading role. The major parts of an aircraft are an engine and wing; both are sensitive parts which lift and propel an aircraft to reach its destination from the airports. wildlife is dangerous, mostly the bird attacks on the aircrafts. Bird collision is a significant threat to civilian and military aircrafts. The leading edge (is the front edge of the main wing), horizontal or vertical stabilizer, which has many considerable roles to be played throughout the flight. The main wings carry the aircraft fuel. The aviation safety concern is bird strikes because of rising air traffic density and increasing floating birds' migration routes[1] and some airports are not located on the very suitable places so there are high chances of birds' collision during takeoff and landing. [2]. The Leading Edge also meet the essential protection criteria to secure the wing. In Part 25 of the Federal Aviation Regulations, an aircraft required, if the aircraft's velocity relative to the bird along the flight path of an aircraft is (Design Cruise Velocity) at sea- level, to be able to complete a flight where the collision with a 4 lb (1.82kg) bird (8lb (3.64kg)for a structure of an empennage) may have structural damage but does not penetrate inside of the wing. The regulations standards of the European Aviation Safety Authority (EASA)(CS-25) have also contained related criteria to the FAR[3], [4]. when a bird strike on the

wing, it acts like a fluid because a young bird contains about 80% to 90% fluid out of his total body weight. Due to water, The bird modeled by using the Murnaghan equation of state (EOS), which has a relationship between volume and pressure by using the Smoothed Particle Hydrodynamics (SPH) method to analyze the impact on the aluminium plate[5]. To explain the resistance of the thermoplastic wing leading edge to the bird's collision to it and the analysis of lightweight material[6]. When designing a wing, we must know about the bird's behavior and the failure mechanism of the structure. Vijaya, Sayyad studied the action of the bird and the failure of the structure[7], [8]. Tim, B. Arachchige explores the collision of a high-velocity strike on the composite materiel leading edge and plate to analyze the characters and the penetration of striking object [9], [10], to avoid the penetration in the wing leading edge thicker honeycomb skin is better to resist to the impact of bird[11]. Competition in the airline industry, every organization tries to explore more economical and safer means of travelling. During designing, the aircraft wing must be lightweight, and its Structures must be capable of bearing bird strike. Vijaya Kumar R. studied the damage of composite Structures during the bird strike by using finite element analysis[12]. For a decent understanding, it is needed to analyze the characteristic of a bird strike on the wing. For that, Cătălin PÎRVU is applied to three different weight 170g to 12kg to get the damage assessment by using the finite element analysis (FEA) [13]. In order to analyze the kinetic energy (K.E) Dahai studied the loss of K.E of the bird during its collision and deformation with the aircraft[14]. To a wide verity of composite material, Every material has a different resistance against the collision. Michael May conducted a study on the high-velocity collision of a bird[15]. Leon researched on the relationship of damage and structure under the tensile and compression lodging[16]. J.Zhou investigated experimental by using FEA high-velocity collision on soft aircraft material like rubber[17]. Saiaf did an analysis of the bird strike on the leading edge of the wing. Depending on the affected prototypes, the aluminium wing is found to be more efficient keeping in view bird collision with the composite wing[18]. Jun has used the SPH method for the 4Ib bird strike on composite Radome structure[19]. His result showed that structure is safe for 4 Ib bird collision. M.L. is a simulated bird strike problem by using practical finite element analysis (PFEA) method[20]. In Abaqus / Explicit, the primary Eulerian computational power enables efficient simulation of fluid flows and massive substantial deformations. By integrating this technology's strength with the conventional Lagrangian method, the complex physics-based processes such as fluid-structure relationships can be replicated where actively deformable structures interact with relatively rigid objects. A. Ajin, M. Guida used Lagrangian approaches to examine the effect of bird strikes on the parts of the aircraft and related the result with (SPH)[21], [22]. CEL approaches normally use large deformation that occurs at high velocity. David J. Benson designed the hydrocodes for Lagrangian and Eulerian[23]. The Salvatore Use CEL methodology to investigate structural deformation and damage development and its spreading by observing specific places of impact and various angles of effects[24] As far as, there is not much research that investigate the bird collision with the composite materials of a wing skin its penetration powe in the wing. In this study, we took the 200m/s velocity of a bird and collided with three different designs. In these three designs, model test A and model test B has a skin and leading-edge is made of unidirectional fiber-reinforced composite material, in model B, it has different shapes of spar and the model test C has an aluminium leading edge other structure is similar to that modal B. Analyze the deformation due to the impact of a bird strike, Brid behavior on the leading edge and after the failure of the leading-edge , bird impact on the spar and inner structure. In this study, we used the CEL method to analyze it and Compared the kinetic energy K.E and internal energy I.E graph at different velocities. The first section is of the bird collision theory. The Second is the bird modeling, the third is the materiel damage model in the fourth is

wing structure, the fifth is test model, the sixth is simulation approaches and the last one is result and dissociation.

Bird impact theory

Mostly the event of impact dived in three categories of theory. The first is elastic impact theory the second is plastic impact theory and the third is hydrodynamic impact theory. These theories are classified based on the impact of velocity. In this study, birds behave like a fluid, so Hydrodynamic theory treated with the fluid. When a bird collides with a body, there is a common characteristics in the pressure background which gets determined by transducers away from the impact of the center but the pressure amplitude gets decreased with increasing radial distance from the impact center. To calculate the time which bird takes to travel through its length and it is expressed by logically as

$$T = \frac{L}{U_B}$$

where L is the length of the bird, T is the duration of impact, and U_B is the initial impact of velocity. In this time duration impact of bird is categorized into four categories as shown in Fig. 1

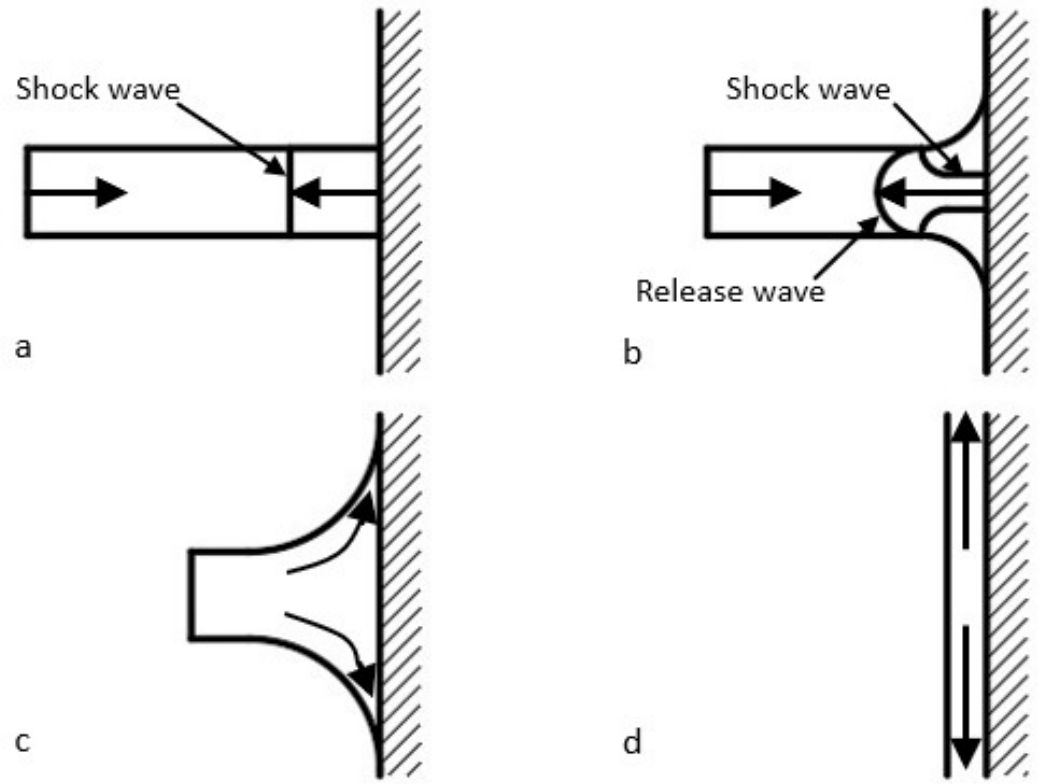

Fig. 1 a) Initial impact b) release shock waves c) study flow d) pressure decay

At first, impact on the part when particles of the front edge of the bird attack on the rigid body. According to newton's third law, it makes an impact on the bird and produces the shock wave according to the hydrodynamic theory by James **S.** Wilbeck cylindrical bird impact on a rigid body[25]. The particles of a bird are at an absolute velocity at the same time when particles of the rigid body collide with a rigid body. Then it produces the shock wave as shown in Fig. 1(b). According to newton's law, the particle of bird gets a reaction and the velocity of reaction is less than the energy of birdparticles before collision because some of energy gets depressed. The smooth way of describing the law of conservation from shock state to bird addressed in Fig.2(c)

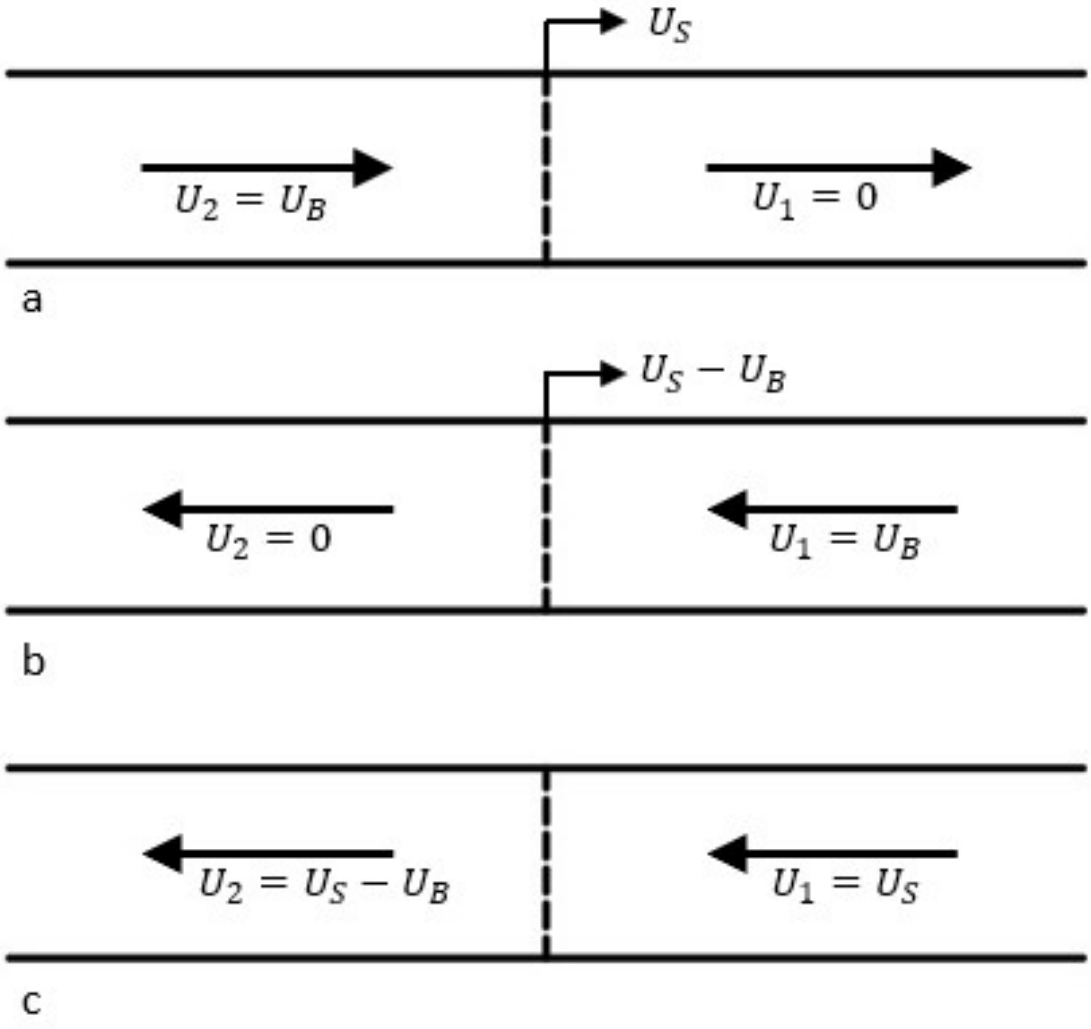

Fig.2

$$\rho_1 U_s = \rho_2 (U_s - U_B) \quad (1)$$

$$P_1 + \rho_1 U_s^2 = P_2 + \rho_2 (U_s - U_B) \quad (2)$$

To found the pressure, combine these two Eq. 1 and Eq. 2

$$P_2 - P_1 = \rho_1 U_s U_B 3$$

In the above equation 3 ρ_1 is the initial density of the bird, U_s is the shock velocity and U_B is the impact velocity. When the impact velocity is low, the shock velocity U_s can be approximated by the velocity of sound in the material. The incompressible Hugoniot (shock) pressure P_H is then it calculate by:

$$P_H = P_2 - P_1 = \rho_1 C_0 U_B \quad 4$$

For the bird impact of velocity, the shock wave U_S is the estimate which is equal to wave velocity of material C_0. Here, if the bird is made of water then $C_0 = 1.4829\text{E}{+}3\, m/s$.when initial shock wave, then the released wave goes to reduce the radial pressure difference to dissolve the impact pressure. Released wave merges at the constant center pressure which are formed by many reflections of the released wave. The velocity of the initial release wave is the same as of the velocity of sound in the shocked material, C_r at the Hugoniot state, it calculated by

$$C_r^{\,2} = \left(\frac{dP}{d\rho}\right)_{P_H} 5$$

If the distance to the center is a and then the duration of the shock wave is

$$t_H = \frac{a}{C_0} 6$$

Eq. 6 shows the time of the released wave to reach the center. The slope of the Hugoniot Condition isotropic pressure-density curve. The end of the particles eventually hit the target, and pressure gets decreased.

Bird modeling

In this, we are using birds, which strike on a wing at a velocity. usually the birds' body have approximately 80% of the water 10% is an another fluid in his body; it means that birds carry the fluid. Most birds fly at high altitudes when when they are to migrate to the long distances. Typically, the bird body temperature is 106 degrees Fahrenheit. However, when it flies on the long routes, his body temperature gets increased approximately by 4 degrees. It goes to 110 degrees Fahrenheit at this temperature density of 990 kg/m^3. When birds fly, they fold their legs, and they look like a cylinder that has ended in Samisphere. The bird acts like a fluid during collision and is designed as a cylinder made of water, but as there are cavities and internal organs containing air, the bird commonly made up of 90% fluid and 10% air. Here in geometry, which represents a real bird which is also in cylindrical shape, and has both ends, is the Samisphere. Here are used empirical formulas which are derived by the Australian Transport Safety Bureau, 2002 [26]. Federal Aviation Regulations which certification required 4Ib bird here bird is also is 4Ib

$$bird\ mass = 4\ IB = 1.82\ Kg$$

$$Density = 959 - 63 * \log_{10}(mass\ of\ bird) = 942.7\ kg/m^3$$

$$Diameter\ of\ bird = 0.0804 * mass\ of\ bird^{0.335} = 0.098\ m$$

$$Length\,of\,bird = 4 * \left[\frac{mass\,of\,bird}{\pi \cdot density \cdot Diameter\,of\,bird^2} - \frac{Diameter\,of\,bird}{6} \right] = 0.189\,m$$

$$Total\,length\,of\,bird = 0.098 + 0.189 = 0.287\,m$$

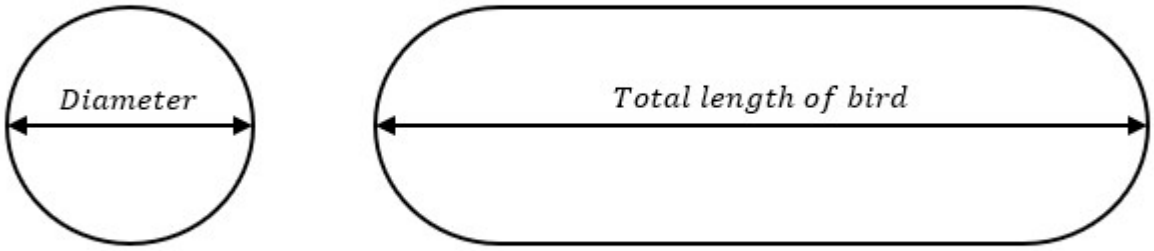

Fig. 3 Bird shape

Our birds carry most of the their weight which is mostly fluid; so we consider hydrodynamics response for a valid approximation for the model. The equation of state has a relationship between volume and pressure at room temperature

$$P = f(\rho, E_m) \qquad 7$$

P is representing pressure, ρ represents density, E_m is representing internal energy per unit mass, if it is written in the form a state Eq. (7) it is said to be linear in energy

$$P = f + g E_m \qquad 8$$

Hence Mie-Grüneisen equations of state (EOS) which describe the relationship between pressure and volume. U_s shok velocity and U_p particle velocity has a linear relationship to define C_0 the velocity of sound and Material constant.

$$U_s = C_0 + S U_p \qquad 9$$

$U_s U_p$ was adopted the approaches in Abaqus/Exiplet of our purpose. Bird marital define in Table 1

Table 1. Material Properties of the bird.

Properties	Values
ρ (kg/m3)	**942.7**
Γo	**0**
Co (m/s)	**1480**
S	**0**

Marital damage modes

Here we conduct our research on the high-velocity collision of the bird on the wing by using FEA. In composite material, three forms of damage are considered: fiber loss, ply fracture delamination. The implementation of an acceptable failure parameter and constative equation to the model the structural characteristics of marital unidirectional fiber-reinforced composite and metal. In this research, the inner structure made by aluminium, and skin is composite materials and simulate our study by using the J-C damage model for aluminium, and Hashin's law is for the unidirectional fiber-reinforced composite material. These both damage model can predict the behavior of material and both available finite element (FE) tools to model the material forming simulations

Damage model of metal

The Johnson-Cook model is a way of analyzing the statistical power and mostly it is used in modeling and simulation work [27], [28]. The Johnson-Cook material model is a universal material relation for metals that are commonly used in impact simulation and problem-related penetration. It has a wide range of potential application. The strength is mostly because of the simple structure and the relative consistency of the pattern constants. Several tensile tests are usually enough to determine the five constants under various loading conditions. A sophisticated and dynamic mechanism involving high plastic strains often requires metal disruption and break up under impact loadings. The substance model of Johnson-Cook (J-C) is commonly used for predicting effect and penetration issues. The feasibility of the J-C model to predict complex content performance and affect load failure. Johnson-Cook model describes the relationship between stress and strain under the condition of large deformation high strain rate and elevated temperature

$$\sigma=\left(1+C\in\varepsilon^{r}\right)\left(1-T_{¿}^{m}\right)\left(A+B\varepsilon^{n}\right)10$$

A, B, C, m, and n is material constant. A is the yield stress, B and n are the parameters of strain hardening, m is thermal constant, $T_{¿}$ is the temperature which is defined

$$T_{¿}=\left(T-T_{r}\right)/\left(T_{m}-T_{r}\right) \qquad 11$$

In which T is the temperature of deformation T_{r} is a temperature of the room, T_{m} is the temperature of the melting point of the material. For the simulation model also takes instigation of material damage Johnson and Cook define the damage of material help of this equation

$$D=\sum\frac{\Delta\varepsilon_{p}}{\varepsilon_{f}\left(\sigma,\varepsilon^{r},T_{¿}\right)} \qquad 12$$

$$\varepsilon_{f}=\left[D_{1}+D_{2}D_{3}\exp\sigma\right]\left[1+D_{4}\in\varepsilon^{r}\right]\left[1-D_{5}T_{¿}\right]13$$

$\Delta\varepsilon p$ is equal to plastic strain in a combination of series σ is to define stress normalized by P pressure and σ_{eff},effective stress is

$$\sigma=P/\sigma_{eff} \qquad 14$$

D_1 D_2 D_3 constants describe the effect of stress on plastic strain at fracture D_4 and D_5 represent the material fracture sensitivity to the rate of strain and temperature.

Damage model of composite material

The unidirectional fiber-reinforced composite layer is damaged mostly by impact velocity on it. For the impact, that time more than one stress acting on the unidirectional fiber-reinforced composite layers, Hashin's law deals with the different types of the failure models and appraise the failure. According to the Hashin's law [29] which is used to[30] study, these criteria are the developers for the unidirectional polymeric composite layer. It will also be consider the rough calculations which are referred to many types of laminate and non-polymer composite materials. Normally Hashin's applies on two-dimensional approaches for point stress. The Hashin's criteria of failure are related to fiber and matrix failure and involve four failure modes, tensile fiber failure, compressive fiber failure, tensile matrix failure and compressive matrix failure. All equations of these failures are shown below. It is also extended for the three dimensional where it uses to normal transverse normal stress

1. Tensile fiber failure for $\sigma_{11} \geq 0$

$$\left(\frac{\sigma_{11}}{X_T}\right)^2 + \frac{\sigma_{12}^2 + \sigma_{13}^2}{S_{12}^2} = \begin{cases} \geq 1 \, failure \\ ¿\, 1 \, no \, failure \end{cases} \quad 15$$

2. Compressive fiber failure for $\sigma_{11} < 0$

$$\left(\frac{\sigma_{11}}{X_c}\right)^2 = \begin{cases} \geq 1 \, failure \\ ¿\, 1 \, no \, failure \end{cases} \quad 16$$

3. Tensile matrix failure for $\sigma_{22} + \sigma_{33} > 0$

$$\frac{(\sigma_{22} + \sigma_{33})^2}{Y_T^2} + \frac{\sigma_{23}^2 - \sigma_{22}\sigma_{33}}{S_{23}^2} + \frac{\sigma_{12}^2 + \sigma_{13}^2}{S_{12}^2} = \begin{cases} \geq 1 \, failure \\ ¿\, 1 \, no \, failure \end{cases} \quad 17$$

4. Compressive matrix failure for $\sigma_{22} + \sigma_{33} < 0$

$$\left[\left(\frac{Y_c}{2S_{23}}\right)^2 - 1\right]\left(\frac{\sigma_{22} + \sigma_{33}}{Y_c}\right) \frac{(\sigma_{22} + \sigma_{33})^2}{Y_T^2} + \frac{\sigma_{23}^2 - \sigma_{22}\sigma_{33}}{S_{23}^2} + \frac{\sigma_{12}^2 + \sigma_{13}^2}{S_{12}^2} = \begin{cases} \geq 1 \, failure \\ ¿\, 1 \, no \, failure \end{cases} \quad 18$$

5. Interlaminar tensile failure for $\sigma_{33} > 0$

$$\left(\frac{\sigma_{33}}{Z_T}\right)^2 = \begin{cases} \geq 1 \, failure \\ ¿\, 1 \, no \, failure \end{cases} \quad 19$$

6. Interlaminar compression failure for $\sigma_{33} < 0$

$$\left(\frac{\sigma_{33}}{Z_C}\right)^2 = \begin{cases} \geq 1 \, failure \\ ¿\, 1 \, no \, failure \end{cases} \quad 20$$

here, the T and C subscriptions show the stress components, and the tensile and compressive strengths, allowed for the lamina. X_T, Y_T, Z_T denote permissible tensile strengths in three material directions, respectively. Moreover, X_C, Y_C, Z_C represent permissible tensile capacities in three principal material directions. Furthermore, in the associated primary external factors directions, S_{12}, S_{13} and S_{23} signify permissible shear strengths. Each criterion for initiation of damage shall attribute to an output component, i.e., fiber strain, fiber compression, epoxy matrix stress, or epoxy matrix compression. The

successful stress is the tension of the destroying environment which can overcome the resistance of internal forces.

wing structure

The most modern aircrafts have a similar wing structure. Through its basic form, the wing is a structure consisting of spars and ribs coated with metal. Wings generate lift to meet the following criteria of a heavier aircraft's lift. Wing systems bear some of the heavy loads found in the construction of an aircraft. The actual configuration of a wing depends on numerous parameters, such as aircraft size, weight, velocity, climb rate, and its uses. The wing must be constructed by keeping in view its aerodynamics profile under the thrilling stresses of struggle exercises or wing loading. A full wing system is consisted of a structure that provides a lift to an aircraft as an assistance. it also provides the appropriate properties for control systems.

WING DESIGN

On a wing, when a bird attacks the leading edge, then the leading-edge becomes failed and bird gets penetrated into the wing and it will ultimately effect the spar. Spar is the central part of a wing. It starts from the aircraft's body, and it goes to the end of the tip of the wing. Spar is used to give the high strength to the combined wing. It usually carries all of the load and stresses. It also provides support to the rib, which is designed to give an aerodynamic shape to the wing, and it is used to attach the wing and the other parts of the wing of an aircraft and it also transmits the air lode to spar. long and narrow wings provide further stability to an aircraft. The downside is that condition in which aircraft would not be more maneuverable. (It is a little bit like a tight rope walker that carries a long pole around the body when walking around the ground – the additional 'arm' lengths help support the body by adding more bulk to both sides of it.) There is also less chances of an induced drag in long and narrow wings than short and broader wings. Drags are produced on the tips the wings, at high-pressure of flowing air from below the wing into the low-pressure area through the wingtips. This place, with different air pressures, transforms it into a turbulent environment which induces induced drag. To get the realistic result, the part of the wing which is near to the plan, its one side rib is free because it is near to the body while the another side of the rib has a long wing and it is vulnerable to the bird strikes on the wing rib under the forces of skin. The other part which is not under the bird strike fulfills these criteria by using coupling connector of all forces combined at a point which is center of the rib as shown in the Fig. 4(a). Replace the other wing with bushing which has elasticity forces on all axis is 1500 N/m and the moment is 4500Nm as shown Fig 4(b).

Other end of wing is under the boundary condition and it is fixed

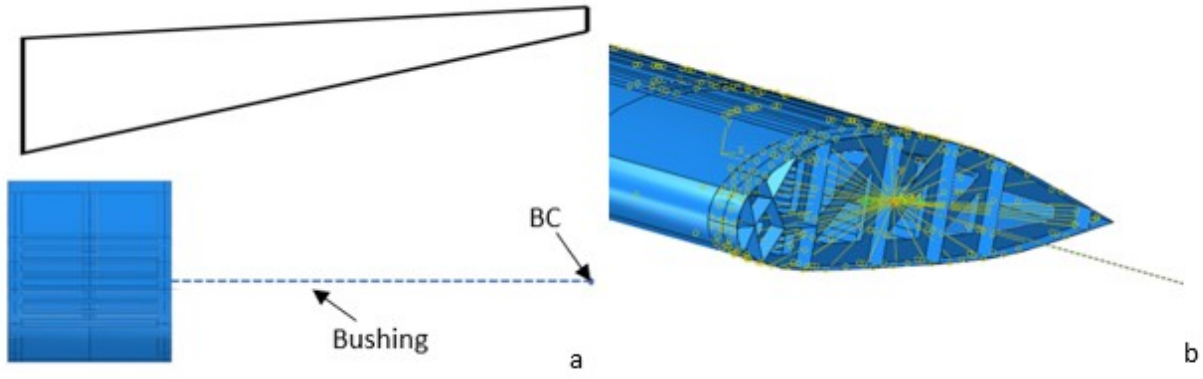

Fig.4

In this study, the wing is under the bird impact. The sub rib is lying in between two ribs of a wing. These two ribs have 0.6m distance between them and the sub rib is center of these two ribs as shown in Fig. 5 The modern aircraft does not need a very long wing. It needs a more substantial wing that can sustain under high acceleration. Between to ribs, a sub rib is provided more strength to spar.

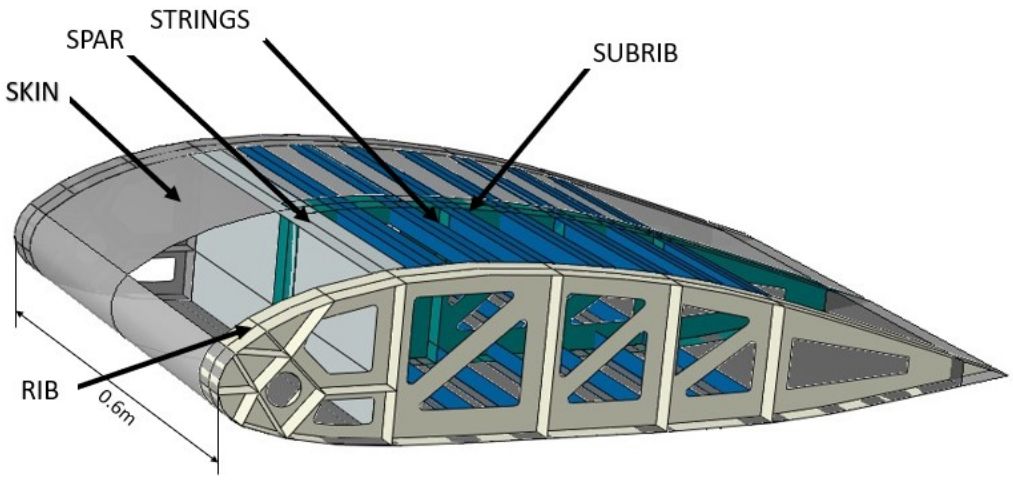

Fig. 5

Furthermore, in this study, three different types of wing under the bird impact were investigated. In the First model wing, the whole skin is with the leading-edge, the second has a different shape of the spar. The third is similar to previous two but just has the plates, and it also has an aluminum leading edge. the thickness of parts shown in table 2

Table no. 2 Properties of parts

Parts	material	Layers of material	The thickness of each layer
Spar	Aluminum	1	0.004m

Rib	Aluminum	1	0.003m
Sub rib	Aluminum	1	0.002m
Strings	Aluminum	1	0.002m
Leading-edge	Aluminum	1	0.002m
Skin	Composite	12	0.0003m
Plates of spar	Aluminum	1	0.004m

Material

Material has a wide range of variety having different properties, in the binging the aircraft wing made with wood. After some time, the aluminum metal has replaced wood in construction of wing. Steel, aluminium, titanium and their alloys are metals which are being used in manufacturing of aircraft. the aluminium alloys have low density values with high corrosion resistance properties as compared to steel alloys (about 1 third). Currently material of the wing making is aluminium 2000 series. Specify 2024 as this alloy contains 0.6% manganese 1.5%magnaisham 4.5%copper, and some other element and rest of composition is aluminium. If we use some other material, then it must be capable of getting the same characteristics of aluminium and it also to be lighter in weight. Composite material is lighter than aluminium—The integration of various materials that were chosen based on their structural properties produces composites. These are made of fibrous materials that mixed into a resin matrix. In general, in order to achieve the necessary strength and rigidity, fibers are aligned in a specific direction and it is laminated by using fibers of different orientations. Composite materials are used primarily for the construction of new aircraft and its use is increasing day by day. Since Last a few years, the use of metallic materials in construction of aircrafts has declined. Mostly composite materials are being used in the aircraft wing skin. It is much lighter than aluminium. It is more capable against the collision resistance. In This study, most of the part is made of aluminium, which is shown in table no. 2 and its properties are shown in table no. 3[31] and its skin is made of unidirectional fiber-reinforced composite material, and its properties are shown in table no. 4

Table NO. 3 Properties of aluminium [31]

Material properties	Value	Material properties	Value
ρ (kg/m3)	2750	Tr (k)	293
E (GPa)	72.2	Tm (k)	775
μ	0.35	D1	0.112
A (MPa)	369	D2	0.123
B (MPa)	684	D3	1.5
c	0.0083	D4	0.007
n	0.73	D5	0
m	1.7		

Table NO. 4 Properties of unidirectional fiber-reinforced composite martial

Material properties	Value	Material properties	Value
ρ (kg/m3)	1570	Longitudinal tensile strength	1665(MPa)
E1	127500(MPa)	Longitudinal compressive strength	1362(MPa)
E2	9000(MPa)	Transverse tensile strength	80(MPa)
Nu12	0.28	Transverse compressive strength	232(MPa)
G12	4900(MPa)	Longitudinal shear strength	61(MPa)
G13	4900(MPa)	Transverse shear strength	61(MPa)

G23	3600(MPa)	Longitudinal tensile fracture energy	12000
		Longitudinal compressive fracture energy	10000
		Transverse tensile fracture energy	1000
		Transverse compressive fracture energy	2000

test models

The fowling study describes the damage of the high-velocity bird collision on the wing because the modern aircrafts are faster than the previous decade's aircrafts. After all, the aircraft is faster than the need for the wing, which is more reliable and lightweight. It needs analysis of strength and failure by experiment. However, experimentation is costly. After one experiment, the wing becomes useless and it is unaffordable for the middle-level organizations. The alternative of this experimentation is FEA like ABAQUS/Explicit, which is suitable for research. It provides a nearly accurate result of the experiment. This strategy is carried out by using Abaqus FEA which is the CEL approach. CEL is the best way for analysis fluid problems and penetration problems. in our study, which is an analysis carried out at 200m/s velocity, on three different models of wings analysis the bird's behavior on the wing and failure of the skin impact on the spar. Our first model test A, in which the wing is similar to that wing which is described wing design part of paper, the inner structure made by aluminium and tied from surface to surface and skin is made of composite material as shown in Fig.6. The second model test B is similar to first one, but spar design is different, as shown in Fig.7. It is designed with horizontal plates like a comb structure, which is helpful to observe the K.E. of the bird. The third model test C is similar to the second model. The difference in the third model is the addition of an aluminium plate on the one of the leading edge, which is shown in Fig.8. In all these tests model birds 4Ib collided on the wing and all of these, we analyzed the K.E. and total energy. After impact analysis, the bird's behavior stress on the skin and ribs. The Damage of composite skin analysis the damage of spar, stress, stress also on sub rib on different time intervals at 200m/s bird strike unidirectional at 180 angle between wing and bird is carried which is shown in Fig 6,7,8

Modal test A

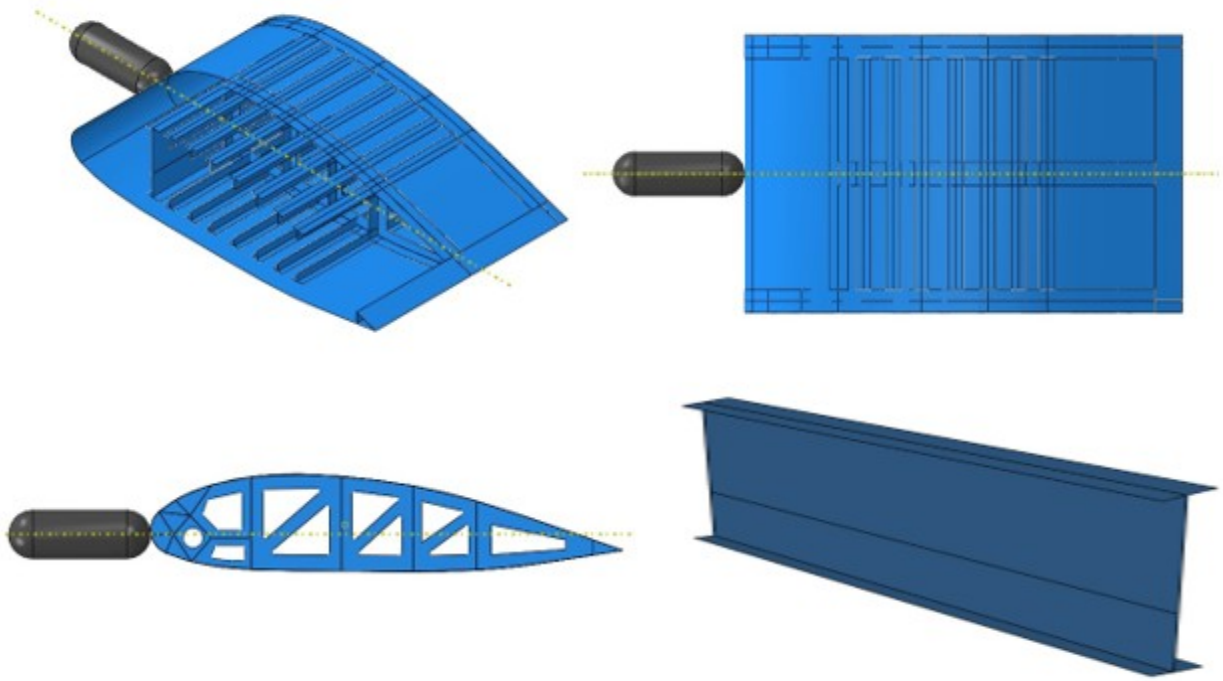

Fig.6
Modal test B

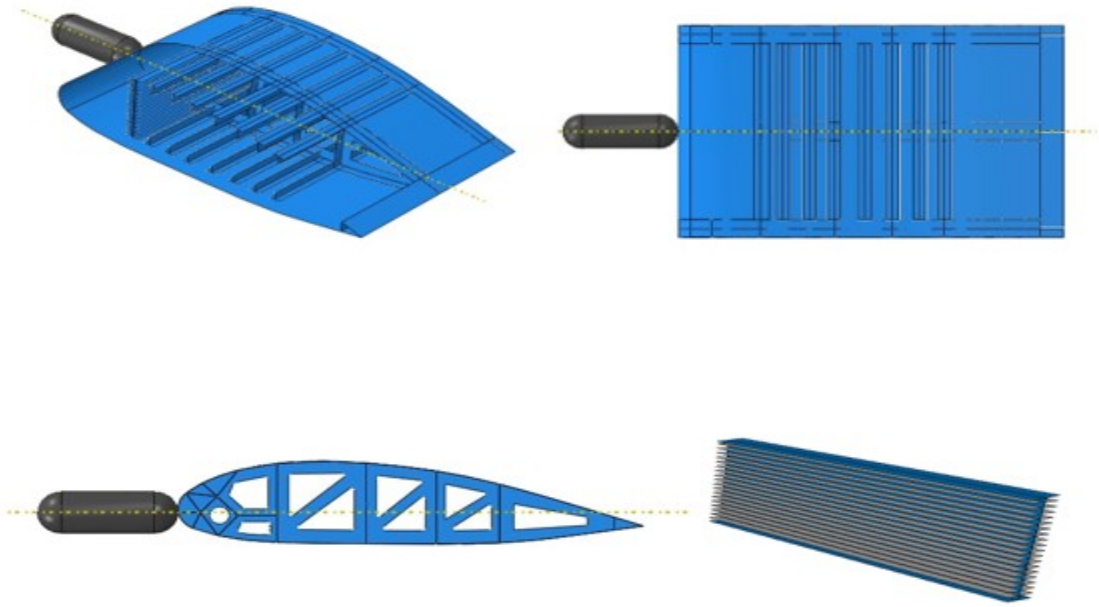

Fig.7
Modal test C

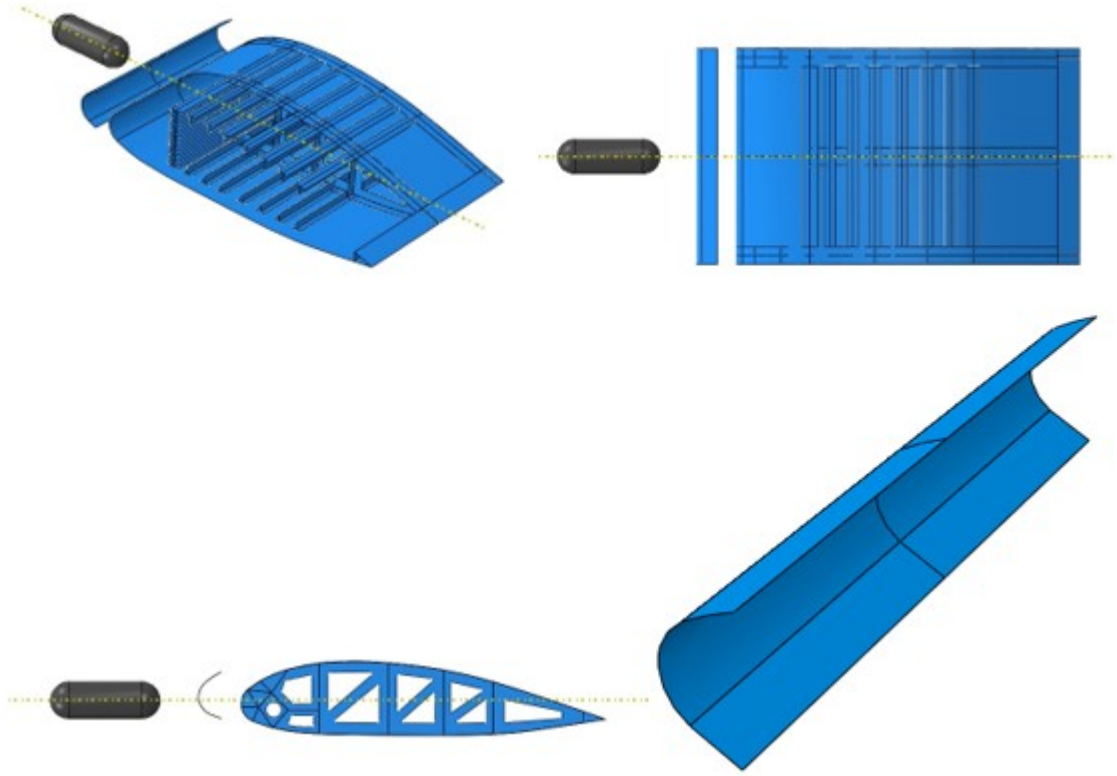

Fig.8

simulation approaches

Four models, such as Lagrangian, Eulerian, Coupled Lagrangian-Eulerian (CEL), and Smooth Particle Hydrodynamics, are currently available and are being used in impact damage analyses. In this survey, we used Coupled Lagrangian-Eulerian (CEL). Each methodology has its strengths and weaknesses.

Coupled Lagrangian-Eulerian (CEL)

A CEL is a m method which is a sheltered the advantage of two techniques is Lagrangian and Eulerian are computed together in Abaqus. Lagrangian and Eulerian techniques are typically used in significant displacement problems of solid mechanics. Both are having their own advantages and weaknesses. In the Lagrangian approach, nodes are fixed within the material. When the element gets deformed in the simulation process, in this approach single element contained original material means 100% with full material. In Eulerian approaches, nodes are fixed in space, and material flows through the elements. It means that it is not deformed, like the Lagrangian approach. Eulerian is not always made of 100% full of material. It may be partially or entirely void. The lagrangian technique is a very suitable distort element like our bird impact problem, which perhaps gets penetrated in the wing skin. Eulerian is suitable for excessive deformation; it is difficult to depend on variable materiel. In this study, we combine these two techniques and which make CEL approaches in which bird is a fluid, and it will get deformed after collision to wing for its use in Eulerian approaches, and our wing material, which is dependent on the history, then it will get a good result by using the Lagrangian technique. For the CEL method, the meshing task considerably is simplified as the soft projectile needs are needed not to be meshed. Preferably, a uniform and straightforward finite element grid from Eulerian elements is constructed so that in the study, the projectile may remain entirely within the mesh borders. It is done eithe by constructing an unmoving

Eulerian mesh that is sufficiently wide to cover the entire course of the projectile from the start to the end of the study or by constructing a moving Eulerian mesh capable of closing the projectile as it travels through space, expanding and contracting according to ref [24] which is derived numerical history of CEL. In space-time, rehashed material and time derivative, respectively, the Lagrangian and Eulerian equation is expressed. In the following relationship space and material time derivatives can be related

$$\frac{D\Phi}{Dt}=v\cdot(\nabla\Phi)+\frac{\partial\Phi}{\partial t} \qquad 21$$

In eq 21 Φ is represented arbitrary solution variable, material velocity is v.

equation of mass is below

$$\rho v\cdot\nabla+\frac{\partial\rho}{\partial t}=0 \qquad 22$$

Equation of momentum

$$(\rho v\times v)\cdot\nabla+\frac{\partial\rho v}{\partial t}=\nabla\cdot\sigma+\rho b \qquad 23$$

Equation of energy conservation

$$(ev)\cdot\nabla+\frac{\partial e}{\partial t}=\sigma:D \qquad 24$$

In above eq,16 ρ is represented to density, b is represented the forces vector, e is represented strain energy, σ is represented Cauchy stress tensor, D is represented to strain rate

The conceptual model of the Eulerian system of the equation which is obtained by equation 22,23,24 is

$$\Phi\cdot\nabla+\frac{\partial\varphi}{\partial t}=s \qquad 25$$

In eq,25of Φ is represented flux function, S is representing the source term. Equation 26 used to solve the Lagrangian step which is

$$\frac{\partial\varphi}{\partial t}=S \qquad 26$$

Eq 27 is used to solve the Eulerian step which is

$$\nabla\cdot\Phi\frac{\partial\varphi}{\partial t}=0 \qquad 27$$

result and dissociation

In this part of paper, the tree wing model simulate the bird strike on the three-wing model test. The bird strike velocity is 200m/s. Bird strikes on the leading edge of wing. According to the bird impact theory

which is described in the upper part of paper. Bird makes impact on the skin of the wing. Due to high velocity bird has high K. E .it makes impact damage on the wing skin or leading edge. When shock wave are converted into a released wave, the bird tries to flow freely. When birds' front edge is released behind, the rest part of bird has K.E more than the of the shock wave of K.E. It tries to damage the skin or leading edge of the wing if bird's K.E. greater than the absorption power of wing on which it fails. According to the K.E graph which is shown Fig.9 and I.E graph which is shown Fig.10 after impact and passage of time KE gets decreased and the I.E gets increased.

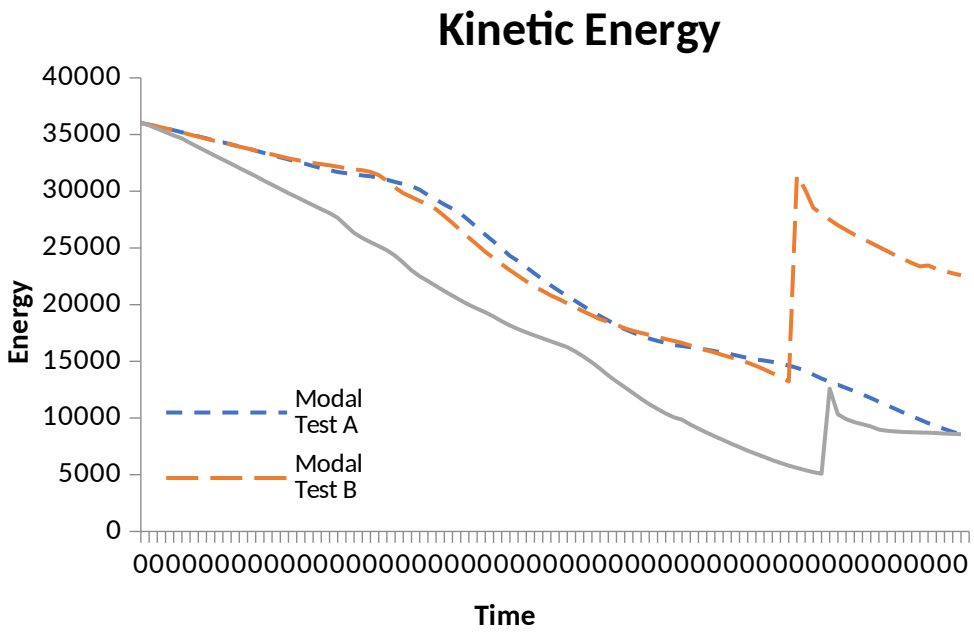

Fig.9

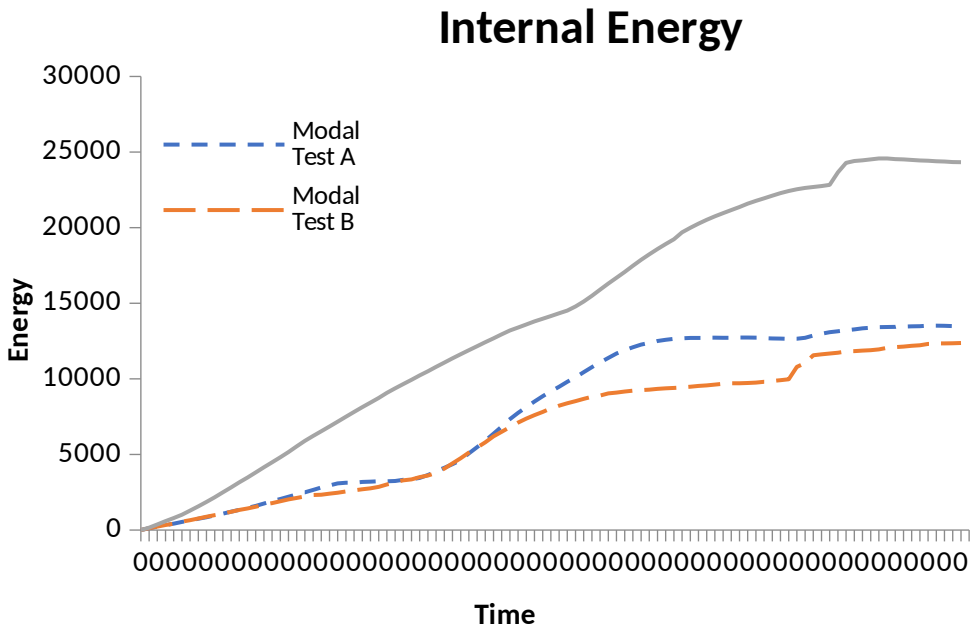

Fig. 10

In wing model A which is leading edge and its skin made of composite material. When a 4Ib bird strikes on the wing at 200m/s. Sami sphere edge of the bird collides with composite skin leading edge which (is shown Table NO. 5 Fig. a) due to high K.E its skin does not absorb the strike of bird and the composite skin gets damaged against the strike of bird. Bird penetrates in the Wing (which is shown Table NO. 5 Fig. c) damages the composite skin along the ribs. After the penetration of that part of bird which is not deformed after collision on the spar. From the front of Sami sphere end edge of bird which is already deformed during the collision with skin. Spar absorb the K.E. of bird and it gets bent from the center along the ribs (which is Table NO. 5 shown Fig. f). Top and bottom plates are also bent towards the center. Due to plates skin is also gets bent inside of the wing. Bird disperses along the surface of spar (which is shown Table NO. 5 Fig. d, f). and bird parts hit the rib makes crake at joining point

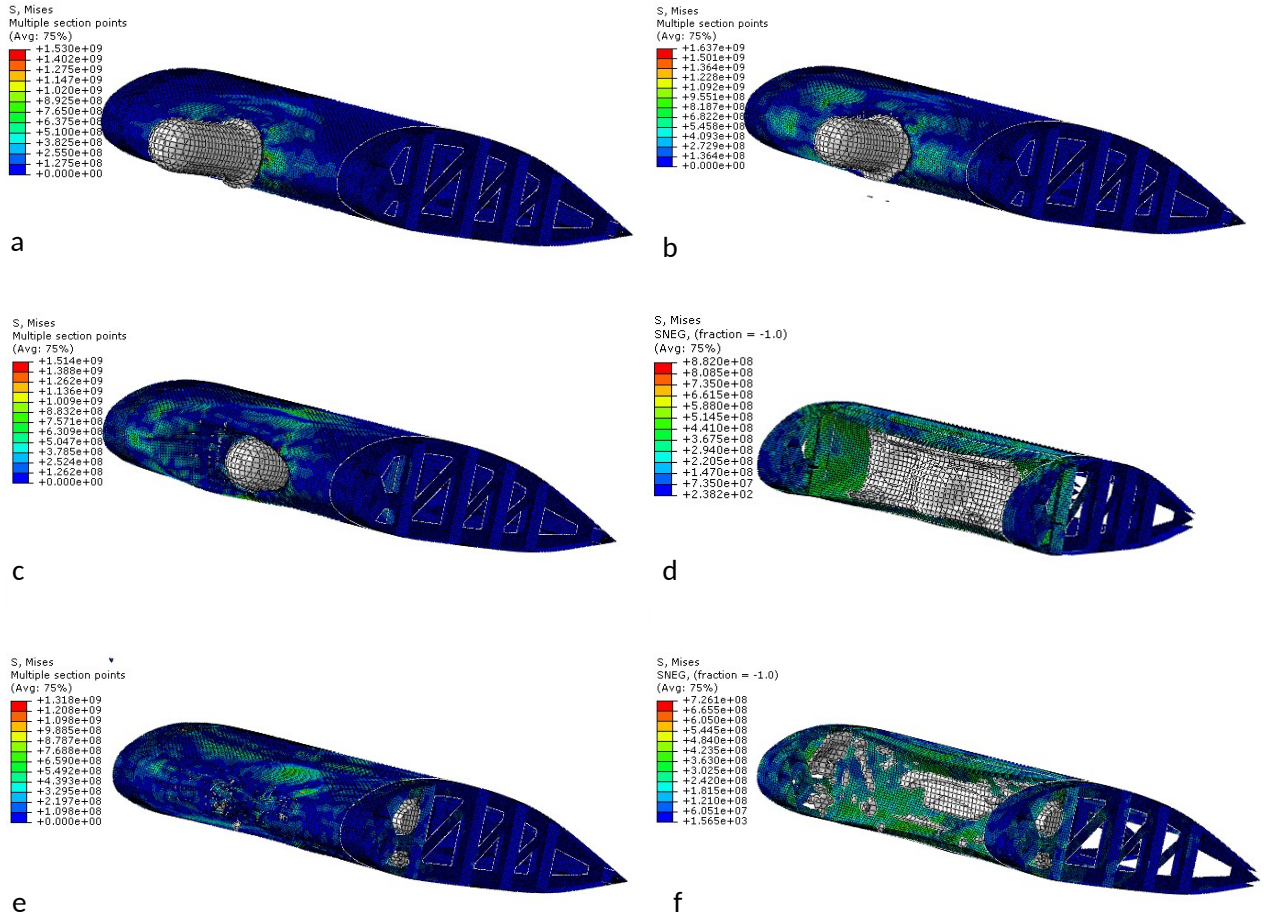

Table NO. 5 Modal A Fig. a) 0.4ms Fig. b) 0.8ms Fig. c) 1.6ms Fig. d) 2.4ms without skin Fig. e) 4ms f) 4ms without skin

In model B which is a similar leading-edge wing model A. But the spar shape is different which is described in the upper part. When in this model wing bird strikes on the leading edge, It gives a similar result to

model A on the leading edge and show an undeform bird impact on the spar. The plates absorb the K.E. of bird and it tries to flow along the surface (which is shown Table NO. 6 Fig. c). spar is less damaged than the model A. When bird collides with plates it tries to cut it into parts. Bird parts flow in different direction and hits the skin and damage it from top to bottom side. The top and bottom plates are also bent towards ribs axis. Skin is bent towards outside (which is shown Table NO. 6 Fig. e). Stress of plates of spar disconnect small parts with rib (which is shown Table NO. 6 Fig. f).

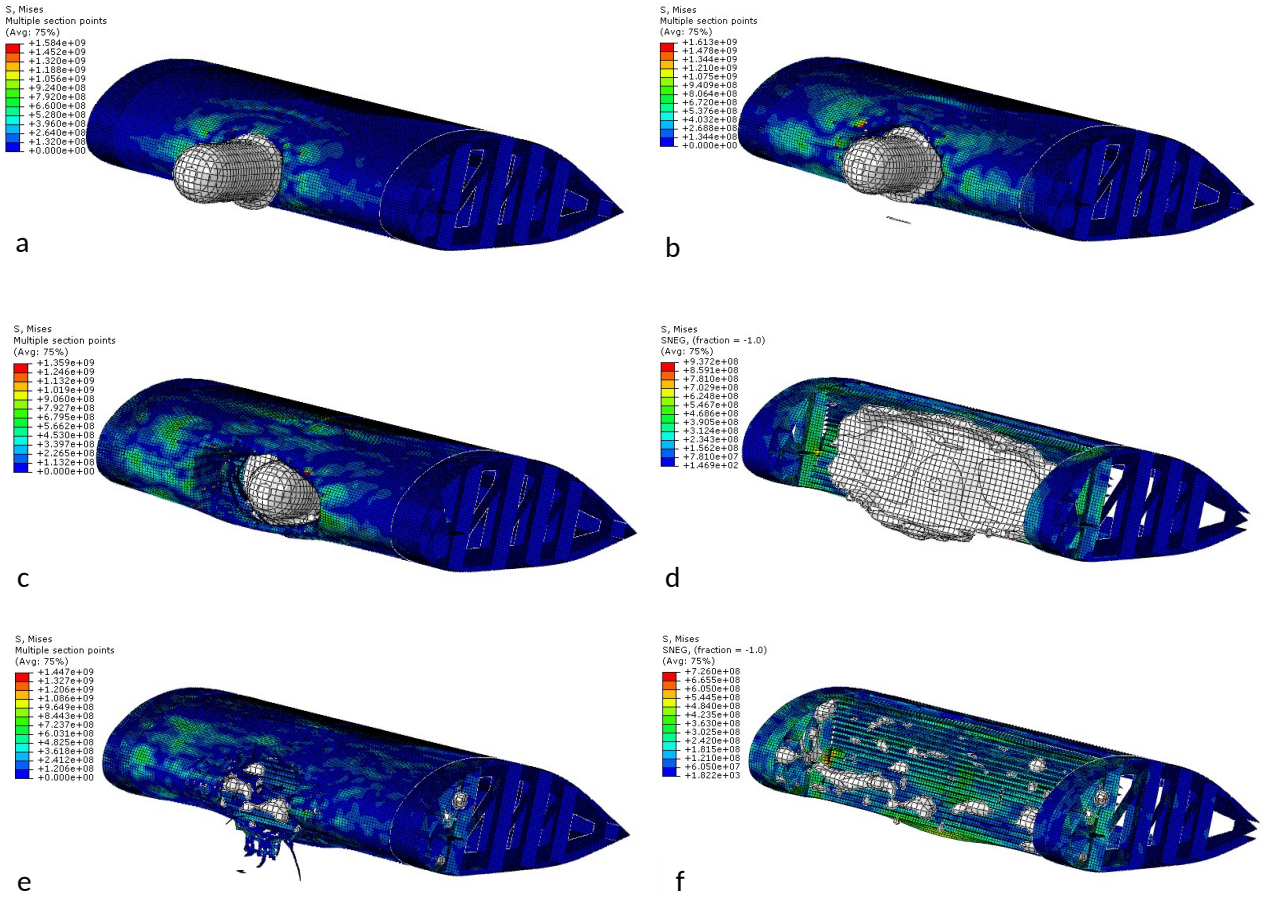

Table NO. 6 Modal B Fig. a) 0.4ms Fig. b) 0.8ms Fig. c) 1.6ms Fig. d) 2.4ms without skin Fig. e) 4ms f) 4ms without skin

In model C which has double leading edge in which the outer leading edge is made by aluminium and other inner structure is same with model B. Each leading edge is fixed from surface to surface with each other. When bird strikes on the leading edge of aluminium due to high K.E. it damages the leading edge and makes bowel shape (which is shown Table NO. 7 Fig. b). aluminium leading edge absorbs the K.E. of bird and it does not penetrate (which is shown Table NO. 7 Fig. d). due to bird's flow on the leading edge which is near to flat outer leading edge. The Outer leading damages the inner leading edge of skin which is made up of the composite material (which is shown Table NO. 7 Fig. e). When bird collides on the leading edge and it pulls rib towards the center which is the side of rib having more part of wing (it is described in

the upper part) that side of rib is not bent and other side of rib is bent towards the center (which is shown Table NO. 7 Fig. d,f). bird also collides on the spar

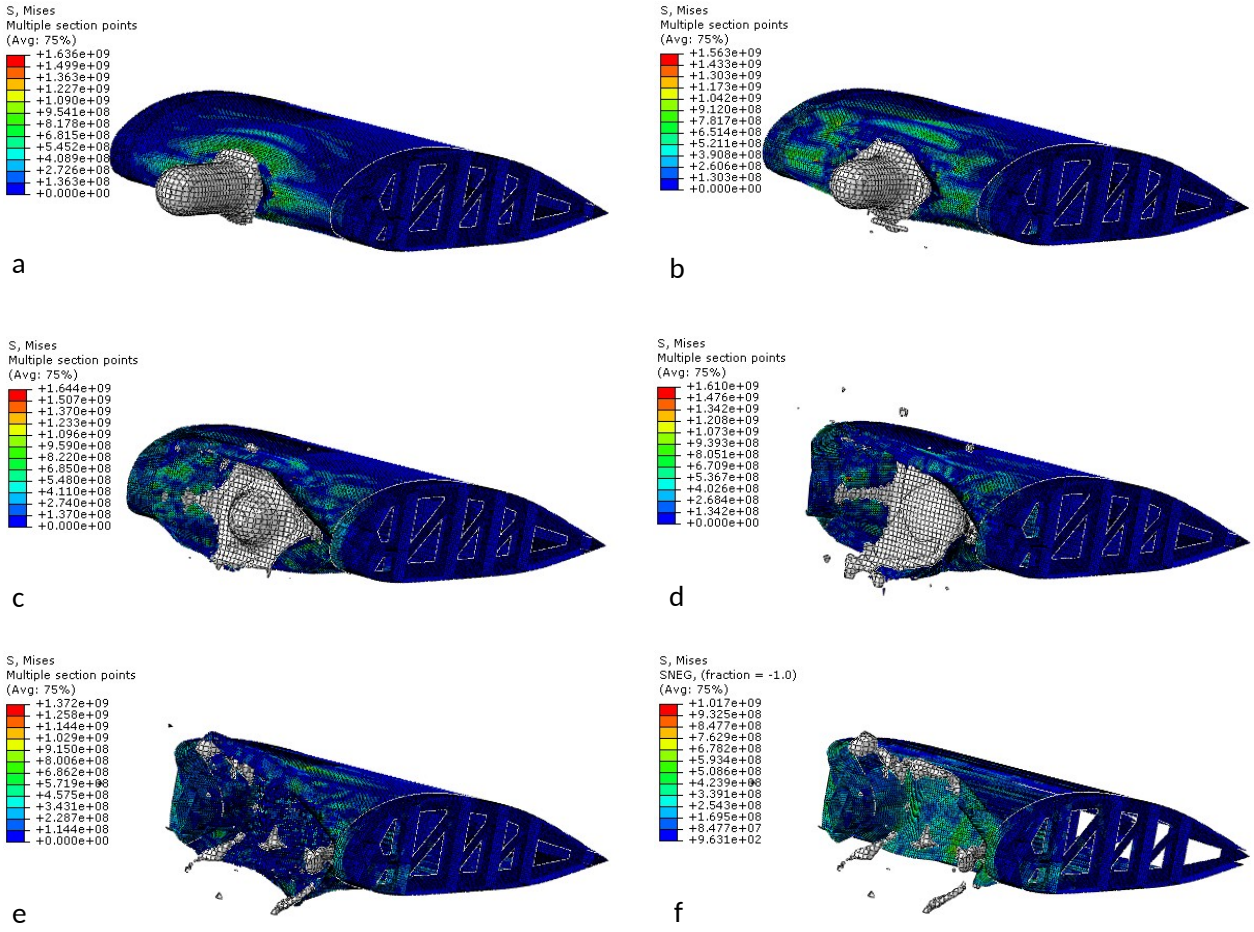

Table NO. 7 Modal C Fig. a) 0.4ms Fig. b) 0.8ms Fig. c) 1.6ms Fig. d) 2.4ms Fig. e) 4ms f) 4ms without skin

We have described the bird impact process on the wings model which shows the details of the whole wing in above part of result section. In this part of results, we are comparing the final the damage of the wing part. First, the fiber tensile which gets damaged on skin demonstrates the weakness in the composite skin after bird collision. In model A skin is damaged along the axis of ribs at the leading edge of skin. When top and bottom plates of spar are bent inside these also damage the skin fiber behind the spar. In model B the skin of wing is also get damaged along the rib axis and when spar plates cut the bird in pieces the same pieces also make fiber tensile damage around the bird penetration area and other places on the composite skin. In model C the whole leading edge of skin is under fiber tensile damage. When the aluminium leading edge becomes damaged due to collision of bird, it makes fiber tensile on skin leading edge of wing. In all of these models wings skin fiber tensile are damaged (show in Table NO. 8 Fig. a). In the second bird collision on the spar it demonstrates the deformation on the spar. In model A spar absorbs the K.E of bird, when it damages like a bowel. In Model B and model C spar plates absorb K.E of bird, the top to bottom side gets bent toward center along the rib of the axis. In Model C spar is less damaged than in model B but it damages in the similar way. All of these spar are shown in (Table NO. 8 Fig. b). in third

ribs and sub rib of wing. Main ribs of model A and model B are damaged nearly in the same manner. The sub rib of both model A,B is damaged in the same manner as to spar damage. In module C one main rib is bent towards the center. The side of which has more part when it is replaced by bushing it is not much bent like other side of rib. All of these spars shown in (Table NO. 8 Fig. c).

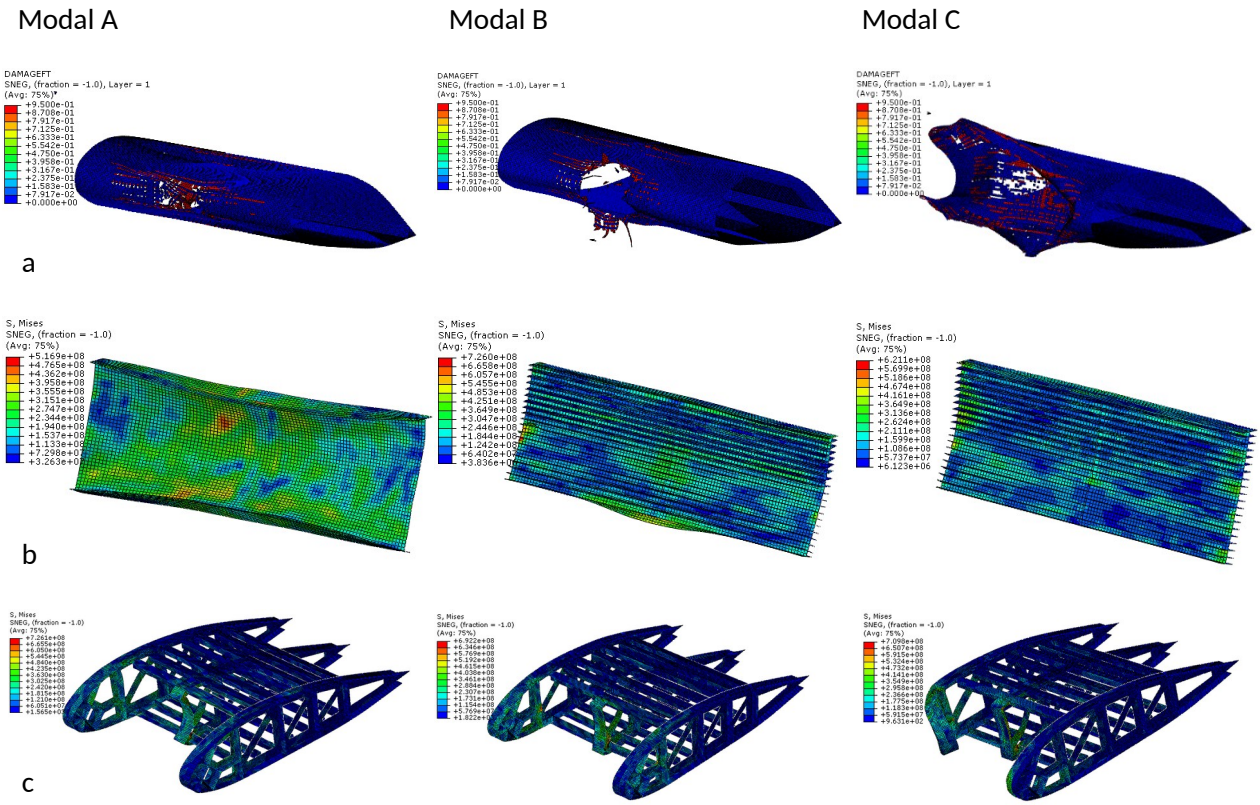

Table NO. 8 a) skin (fiber tensile damage) b) Spar c) Ribs, Sub ribs and strigs

Conclusion

The main aim of this research paper is to analyze the different type of wing molded under the impact at the velocity of bird 200m/s by using the numerical experiment approach, Coupled Eulerian-Lagrangian in ABAQUS/Explicit. In this study the bird is acted as a fluid. Hydrodynamic theory is applied on the bird and bird is molded by using the Eos with the water properties. By Using two materials in the wing of an aircraft is designed. The first material is aluminium which is simulate under the J.C. model and the second one is unidirectional fiber-reinforced composite material which is simulate under the Hashin's damage model. A small part of wing for bird strike is choosed and other part of wing is replaced by bushing the inner structure which is made by aluminium and its skin is also made by aluminium. In second wing model B has different shape of spar as compared to model A. In the third wing model C has a leading edge which is made of aluminium. Based on all experiments, our bird acted as fluid according to Hydrodynamic theory. The skin of all wings is made by composite material which gets fail against the bird strike. Model A wing spar is damaged. If the velocity is high then the spar will fail. Model b wing spar absorbed the K.E of bird and it is able to bear the strike of high velocity. In model C the leading edge is not failed against the bird strike but it destroys the composition of the composite material's leading edge which is fix by surfaces to surface. Due to aluminium leading edge, it bends the rib of one side of the side which has no more wing. This aspect of the research suggests that only the composite material is not able to absorb the strike of a

bird at high velocity. Wing model B spar is more reliable than those of the others. The leading edge of aluminium to fix composite material which is joined from surface to surface put some distance.

References

[1] J. Allan, A. Baxter, and R. Callaby, "The impact of variation in reporting practices on the validity of recommended birdstrike risk assessment processes for aerodromes," *J. Air Transp. Manag.*, 2016, doi: 10.1016/j.jairtraman.2016.07.012.

[2] D.-D. Yang, Z.-Q. Zhang, and M.-W. Hu, "Ranking birdstrike risk: A case study at Huanghua International Airport, Changsha, China," *Acta Ecol. Sin.*, 2010, doi: 10.1016/j.chnaes.2010.03.007.

[3] Federal Aviation Regulations, "Part 25-Airworthiness Standards: Transport Category Airplanes," *Fed. Aviat. Adm. (FAA), USA*, 1989.

[4] EASA, "European Aviation Safety Agency: CS-25," *Easa*, 2018, doi: 10.1002/9780470664797.

[5] J. Liu, Z. Liu, and N. Hou, "An Experimental and Numerical Study of Bird Strike on a 2024 Aluminum Double Plate," *Acta Mech. Solida Sin.*, vol. 32, no. 1, pp. 40–49, 2019, doi: 10.1007/s10338-018-0071-1.

[6] M. Guida, F. Marulo, and S. Russo, "NiTi SMA Wires Coupled with Kevlar Fabric: a Real Application of an Innovative Aircraft LE Slat System in SMAHC Material," *Appl. Compos. Mater.*, vol. 25, no. 2, pp. 269–298, 2018, doi: 10.1007/s10443-017-9618-4.

[7] V. K. Rayavarapu, "On the Bird Impact Damage Assessment of Rotorcraft Horizontal Stabilizer," *Appl. Compos. Mater.*, vol. 26, no. 1, 2019, doi: 10.1007/s10443-018-9703-3.

[8] S. A. Kalam, V. K. Rayavarapu, and R. J. Ginka, "Impact Behaviour of Soft Body Projectiles," *J. Inst. Eng. Ser. C*, vol. 99, no. 1, pp. 33–44, 2018, doi: 10.1007/s40032-017-0348-z.

[9] B. Arachchige, H. Ghasemnejad, and M. Yasaee, "Effect of bird-strike on sandwich composite aircraft wing leading edge," *Adv. Eng. Softw.*, vol. 148, no. February, p. 102839, 2020, doi: 10.1016/j.advengsoft.2020.102839.

[10] T. Wagner, S. Heimbs, F. Franke, U. Burger, and P. Middendorf, "Experimental and numerical assessment of aerospace grade composites based on high-velocity impact experiments," *Compos. Struct.*, vol. 204, pp. 142–152, 2018, doi: 10.1016/j.compstruct.2018.07.019.

[11] F. Di Caprio, D. Cristillo, S. Saputo, M. Guida, and A. Riccio, "Crashworthiness of wing leading edges under bird impact event," *Compos. Struct.*, vol. 216, no. November 2018, pp. 39–52, 2019, doi: 10.1016/j.compstruct.2019.02.069.

[12] R. V. Kumar, "Experiment-based explicit dynamics analysis for bird strike damage prediction in composite structures," *J. Fail. Anal. Prev.*, vol. 18, no. 4, pp. 877–886, 2018.

[13] C. Pîrvu, C. E. Boșcoianu, M. V. Pricop, and L. Deleanu, "BIRD STRIKE DAMAGE ASSESSMENT FOR AN AIRCRAFT TAIL PLANE," *Mech. Test. Diagnosis*, vol. 6, no. 4, pp. 12–21, 2016.

[14] D. Zhang and Q. Fei, "Effect of bird geometry and impact orientation in bird striking on a rotary jet-engine fan analysis using SPH method," *Aerosp. Sci. Technol.*, vol. 54, pp. 320–329, 2016.

[15] M. May, S. Arnold-keifer, and T. Haase, "Composites Part C : Open Access Damage resistance of composite structures with unsymmetrical stacking sequence subjected to high velocity bird

impact," *Compos. Part C Open Access*, vol. 1, no. June, p. 100002, 2020, doi: 10.1016/j.jcomc.2020.100002.

[16] L. Mishnaevsky Jr and G. Dai, "Hybrid carbon/glass fiber composites: Micromechanical analysis of structure–damage resistance relationships," *Comput. Mater. Sci.*, vol. 81, pp. 630–640, 2014.

[17] J. Zhou *et al.*, "Experimental and numerical investigation of high velocity soft impact loading on aircraft materials," *Aerosp. Sci. Technol.*, vol. 90, pp. 44–58, 2019, doi: 10.1016/j.ast.2019.04.015.

[18] S. Bin Rayhan, "Finite element analysis of oblique bird strike on leading edge of aircraft wing," *AIP Conf. Proc.*, vol. 1980, 2018, doi: 10.1063/1.5044288.

[19] J. H. Jang and S. H. Ahn, "Bird-Strike Damage Analysis and Preliminary Design of Composite Radome Structure Using Smoothed Particle Hydrodynamics," *Appl. Compos. Mater.*, vol. 26, no. 3, pp. 763–782, 2019, doi: 10.1007/s10443-018-9750-9.

[20] M. L. Cerquaglia, G. Deliége, R. Boman, L. Papeleux, and J. P. Ponthot, "The particle finite element method for the numerical simulation of bird strike," *Int. J. Impact Eng.*, vol. 109, pp. 1–13, 2017, doi: 10.1016/j.ijimpeng.2017.05.014.

[21] A. A. Kisho, G. D. Kumar, J. Mathai, and V. Vickram, "Effect of bird strike on compressor blade," *Springer Proc. Math. Stat.*, vol. 124, pp. 179–195, 2016, doi: 10.5176/2251-1911_CMCGS14.40_16.

[22] M. Guida, F. Marulo, M. Meo, A. Grimaldi, and G. Olivares, "SPH - Lagrangian study of bird impact on leading edge wing," *Compos. Struct.*, vol. 93, no. 3, pp. 1060–1071, 2011, doi: 10.1016/j.compstruct.2010.10.001.

[23] D. J. Benson, "Computational methods in Lagrangian and Eulerian hydrocodes," *Comput. Methods Appl. Mech. Eng.*, vol. 99, no. 2–3, pp. 235–394, 1992.

[24] S. Saputo, A. Sellitto, A. Riccio, and F. Di Caprio, "Crashworthiness of a Composite Wing Section: Numerical Investigation of the Bird Strike Phenomenon by Using a Coupled Eulerian–Lagrangian Approach," *J. Mater. Eng. Perform.*, vol. 28, no. 6, pp. 3228–3238, 2019, doi: 10.1007/s11665-019-03944-0.

[25] J. S. Wilbeck, "Impact behavior of low strength projectiles (AFML-TR-77-134)," *Air Force Mater. Lab, Dayton, USA*, 1978.

[26] A. T. S. Bureau, "The hazards posed to aircraft by birds," *Unpubl. Rep. Commonw. Dep. Transp. Reg. Serv. Canberra, ACT*, 2002.

[27] R. Neuvonen, T. Skriko, and T. Björk, "Use of the quasi-static Johnson-Cook model in the failure assessment of tensile specimens with metallurgical constraints," *Eur. J. Mech.*, p. 104011, 2020.

[28] H. Zhang, C. Guo, and Y. Chen, "Inverse Material Characterization through Finite Element Simulation of Material Tests and Numerical Optimization," *Procedia Manuf.*, vol. 34, pp. 455–462, 2019.

[29] Z. Hashin, "Failure criteria for unidirectional fiber composites," 1980.

[30] D. H. Kim and S. W. Kim, "Numerical investigation of impact-induced damage of auxiliary composite fuel tanks on Korean Utility Helicopter," *Compos. Part B Eng.*, vol. 165, no. March 2018, pp. 301–311, 2019, doi: 10.1016/j.compositesb.2018.11.117.

[31] Q. Zhu, C. Zhang, J. L. Curiel-Sosa, T. Quoc Bui, and X. Xu, “Finite element simulation of damage in fiber metal laminates under high velocity impact by projectiles with different shapes,” *Compos. Struct.*, vol. 214, no. February, pp. 73–82, 2019, doi: 10.1016/j.compstruct.2019.02.009.